The exploration of the thermodynamics of SNARE complex stability and the automatization of the generation of hybrid topologies

Benjan Karnebeek s3157318

Abstract:

SNAREs are multimeric protein complexes consisting of four chains, they can enable membrane fusion thus allowing for vesicle trafficking between organelles of a cell. Recently four key residues were discovered by *Malmersjö et al.* that retard vesicle fusion when phosphorylated or mutated to glutamate but improve vesicle fusion when mutated to alanine. Here the mutations and phosphorylation of the residues is simulated using thermodynamic integration. This reveals that the mutations and phosphorylation affect the free energy of folding of the SNARE complex thus either stabilizing (for mutations to alanine) or destabilizing (for mutations to glutamate or phosphorylation) the complex, thus either promoting or inhibiting SNARE mediation vesicle fusion. In addition a modified version of pmx program called martini-pmx was made. This version can also make hybrid topologies compatible with the Martini 3.0 force field.

Introduction

Cells of all eukaryotes are divided into compartments called organelles each with their own internal environment and protein content optimized for the function. To exchange compounds between organelles without compromising the structural integrity, vesicles bud from one organelle membrane and then fuse with another[1]. The same mechanism is also used to excrete compounds produced by organelles[1]. This combination of compartmentalization and trafficking in part causes the spatial complexity of higher organisms/eukaryotes[2]. The fusion of the vesicle with the cellular membrane or the membrane of an organelle occurs in 3 steps: 1, docking of the vesicle with the membrane; 2, priming of the fusion machinery on both membrane surfaces and 3, physical merging of the lipid bilayers [1]. This fusion process cannot happen spontaneously, however, as electrostatic and hydrostatic forces cause membranes to repel each other[3]. All three steps in the membrane fusion are thought to be mediated by a protein complex called **S**oluble **N**SF (N-ethylmaleimide sensitive fusion protein) **A**ttachment protein **RE**ceptor or SNARE[1]. The SNARE is a bundle consisting of four helical proteins consisting of one arginine containing helix or R-SNARE, and three glutamine containing helices or Q-SNAREs (Qa, Qb and Qc)[4,5].

The SNARE complex(figure 1) has one ionic and 15 hydrophobic layers of interactions between the different components of the SNARE complex[5,6]. Specific residues in SNARE complexes can be phosphorylated which may either promote or inhibit vesicle fusion[7–11]. Residues which have opposite effects may be phosphorylated by the same protein resulting in an incoherent feed forward loop [12]. VAMP8 is the R-SNARE of the SNARE complex of rats (*Rattus norvegicus*) and mice (*Mus musculus*); the other components are Syntaxin 7 (Qa), Vti1b (Qb)

and Syntaxin 8 (Qc)[6,13]. Recently four phosphorylation sites (T47, T53, S54 and S61) were identified in VAMP8 which completely suppress the function of the SNARE complex when phosphorylated[7]. Residues T47, S54 and S61 were located in the +3, +5 and +7 hydrophobic layers, while residue T53 lies just outside layer +5. The authors[7] proposed this mechanism might function as a general mechanism to reduce synaptic vesicle fusion and thus prevent complete release of all secretory vesicles. Mutating these residues into alanine, and thus preventing phosphorylation, improved secretion in comparison to unphosphorylated WT VAMP8 even if VAMP8 is knocked down. Mutating even one of these residues to glutamate (a phosphomimetic mutation as the negative charge mimic that of phosphate) completely prevents fusion. The mechanism as to how the phosphorylation and mutations affect the vesicle fusion is currently unknown however.

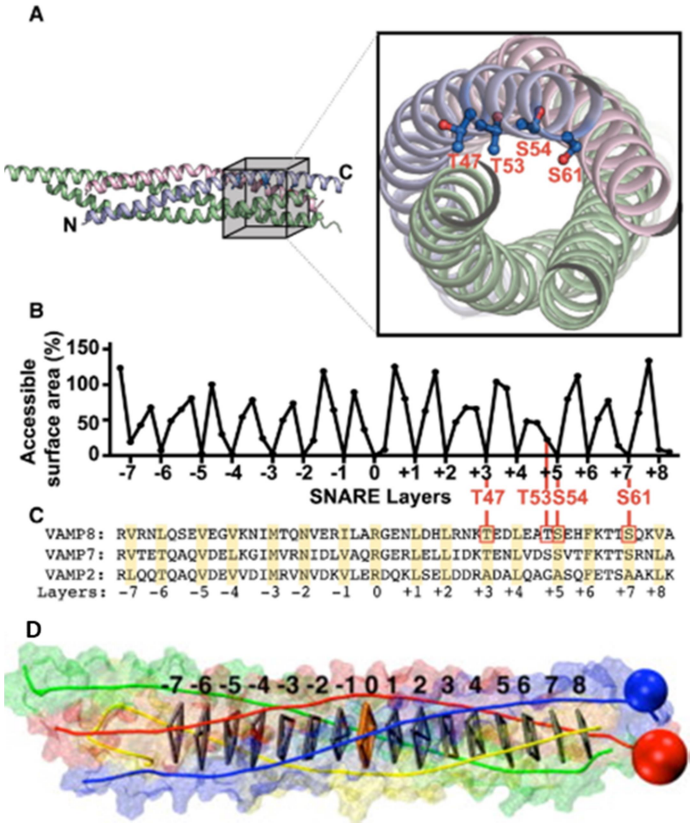

Figure 1: Overview of the SNARE complex **A:** Crystal structure of VAMP8 in an autophagy SNARE complex (PDB: 4WY4). Residues T47, T53, S54, and S61 are shown as sticks-and-balls in the middle of the SNARE complex in an orthogonal view (image retrieved from *Malmersjö et al.*[7]). **B:** Accessible surface area for each residue in the VAMP8 SNARE domain (calculated from PDB: 4WY4). The 16 SNARE layers are all buried inside the SNARE complex with minimal surface accessibility. The four phosphorylation sites (T47, T53, S54, and S61) all have low accessible surface areas (image retrieved from *Malmersjö et al.* [7]). **C:** Sequence of rat VAMP8 SNARE domain compared to VAMP7 and VAMP2 (synaptobrevin). The 16 layers in the SNARE domain are highlighted in yellow and numbered below, with arginine (R) at layer zero (image retrieved from *Malmersjö et al.* [7]). **D:** Visual representation of the SNARE complex with the 16 layers visualized and marked (image retrieved from *Durrieu et al.*[5]).

A recent article[14] used Molecular Dynamics simulations to provide evidence that SNARE mediated membrane fusion is an entropically driven process in which SNARE complexes form a ring pulling the two membranes closer together enabling fusion, after the SNARE complexes have fully zippered. It is therefore a reasonable hypothesis to assume that the mutations and phosphorylation of the residues discovered by *Malmersjö et al.*[7] influence the zippering of the SNAREs by either stabilizing or destabilizing the SNARE complex by altering the free energy released by the zippering. In this study this hypothesis will be tested by performing MD simulations doing thermodynamic integration using GROMACS software[15,16] (specifically version 2018.1) in order to determine whether or not the mutations and phosphorylation of the residues stabilize or destabilize the SNARE complex.

Molecular dynamics (MD)[17,18] is a method for analyzing the physiochemical properties of molecules through computer simulations. In these simulations the Newtons equations of motion are solved for the molecules of the system that is being simulated, the interactions and forces between the particles are given as energy potentials. GROMACS[15,16] is a versatile open source software that can use all major MD force fields including 15 flavors of AMBER, CHARMM, GROMOS and OPLS, and is one of the few[19,20] MD programs that can use the coarse-grained Martini force field[16]. The GROMACS version used here was 2018.1 as it is the most recent version that can be used by the Peregrine HPC cluster[21]. Thermodynamic Integration(TI) is a method to calculate or estimate the free energy difference between two different states of a system by using the free energy difference of both states to a reference state. In this study the TI method described by Seeliger and De Groot[22] will be used to estimate the free energy of folding for both the WT and mutant SNARE complexes using ALA-X-ALA and GLY-X-GLY tripeptides as reference for the unfolded state of the protein. This will be done for both phosphorylation and mutations to alanine and glutamate in order to evaluate the effects of both types of mutations. The mutations will be performed with the new coarse-grained force field Martini 3.0.4[23] in order to test this force field. In addition the mutations will also be simulated using GROMOS54a7[24] and AMBER99sb-ILDN[25] force fields to have fully tested atomistic force fields to compare the Martini 3.0.4 force field to. GROMOS54a7 was picked as a GROMOS force field was used to create the original Martini force field[26,27] and it is the most advanced GROMOS force field compatible with GROMACS 2018.1. The AMBER-99sb-ILDN force field was picked to have another atomistic force field to compare the results of the GROMOS force field to and it is the most advanced versions of the AMBER force field compatible with GROMACS 2018.1. For GROMOS and Martini force fields phosphorylation will be simulated as well. Phosphorylation was not simulated for the AMBER force field because no force field variant with post translational modifications for AMBER force field could be found that was compatible with GROMACS software[28,29].

AMBER99sb-ILDN like other AMBER force fields (as well as most CHARMM[30,31], and OPLS[32]) is an all-atom force field (meaning all atoms are simulated). While AMBER in general is parameterized for protein simulations[33,34], this particular force field was optimized to have secondary structure[34] and side-chain torsions[25] in better agreement with experimental NMR data. GROMOS54a7 like other GROMOS force fields is an united atom force field (meaning aliphatic CH_n groups are combined into singular atoms). GROMOS 54a7 was parameterized for pure liquids of a range of small polar molecules and the solvation free enthalpies of amino acid analogs in cyclohexane with the partial charges adjusted for better hydration free energy and improved torsional angles and charged groups and particles.
The Martini force fields are coarse grained force fields, this means that several (~4) large atoms (e.g. not a hydrogen) along with their hydrogens get combined into a single bead. The Martini force field was originally parameterized for lipids[26] but was later expanded for proteins[35]. The new Martini 3.0.4 force field[23] has two additional bead sizes small (S) beads and tiny (T) which represent 3 and 2 large atoms respectively, these additional bead sizes allow Martini 3.0.4 to capture the differences between the various amino acids better than its predecessors as the smaller beads allow for more details.

The initial simulations showed large difference between the force fields even between the GROMOS and AMBER force fields despite both being atomistic. Thus simulations using different conditions (using a bigger box size for GROMOS and AMBER, using PME for GROMOS and Martini and using ions that shift charge when the state changes for the mutations to glutamate and phosphorylation) were done in an attempt to alleviate the difference in values between the AMBER and GROMOS force fields.

Seeliger and De Groot made a program called pmx[36–39] to automatize the making of hybrid topologies which can be used for thermodynamic integration, thus enabling high throughput TI simulations. This program works

for the AMBER, CHARMM and OPLS force fields. Here a modified version was made called martini-pmx which also works for the Martini 3.0.4 force field thus enabling high throughput TI simulations for a coarse-grained force field.

Materials and Methods

Software:

GROMACS version 2018.1 was used[15,40]. The force fields that were used were GROMOS54a7[24] , AMBER99sb-ILDN[25] and Martini 3.0.4[23].

GROMOS54a7 is an united atom force field in which the bond, angle and dihedral parameters are given as types (e.g. gb_27 for a bond between two CH_n groups)[24,41]. GROMOS normally uses reaction field electrostatics[42].

AMBER99sb-ILDN[25] is an all-atom force field in which the force constants and equilibrium values of a bond, angle, dihedral etc. do not need to explicitly given in the topology as the force field has those stored for all combination of atoms involved in the bond, angle, dihedral etc. that are possible for the force field. AMBER always makes use of Particle Mesh Ewald (PME) electrostatics for simulations[43].

Contrary to the atomistic force fields, for Martini 3.0.4 (as with all Martini force fields[26]) the masses of atoms do not need to be explicitly given while the force constants and equilibrium values of all bonded interactions do need to be fully written out in a topology file. Martini 3.0.4 normally uses reaction field electrostatics[42]. The force field has three bead sizes; normal (represent ~4 Large atoms, mass 72.0 kDa), small (S) beads (represent ~3 large atoms, mass 54.0 kDa) and tiny (T) beads (represent ~2 large atoms, mass 36.0 kDa).

Preprocessing:

The SNARE complex was retrieved from the PDB database (PDB-ID: 1gl2). Missing atoms were added and mutation were made using PyMOL[44,45]. Further preprocessing was done using scripts utilizing GROMACS commands (see supplementary files).
For GROMOS and AMBER: First the structure is energy minimized and then periodic boundaries are added (cubic box for tripeptides, triclinic for SNARE complex but dodecahedron in case of the larger boxes, using a dodecahedron generates a larger box for the SNAREs). Minimal distance between protein and borders is 3.0 nm for tripeptides and 1.0 nm for SNARE complex (otherwise the proteins and tripeptides will interact with a counterpart of itself past the periodic boundary). Then solvent and ions are added to the system, and the system was energy minimized again. Afterwards a short position restrained simulation was performed followed by a short temperature coupled simulation and then a pressure coupled simulation.
For Martini: First martinize2[46] is used to convert a pdb structure to a topology file using Martini coarse-grained beads and force field. The topology file was edited to refer to main, solvent and ions topology files in the martini 3.0.4 force field directory. Then periodic boundaries are added (cubic box for tripeptides, triclinic for SNARE complex), minimal distance between protein and borders is 3.0 nm for tripeptides and 1.0 nm for SNARE complex. Afterwards a short energy minimization run was performed. Then water is added to the system (editing the topology file to make sure the water beads have the right names) followed by another minimization run. Then ions are added to the system followed by a minimization run and a equilibration run.

For the GROMOS and Martini force fields the topology files were manually edited after preprocessing to add the second states(figure 2A). The topologies with the second states are called hybrid topologies. For phosphorylation and mutations to glutamate the phosphorylated residue or the glutamate is used as the first

state. This is done because these residues are larger than unphosphorylated threonine or serine and thus have more atoms in the atomistic models (GROMOS and AMBER), making it easier to construct hybrid topology files for the TI simulations as less atoms need to be added that way (figure 2B). This reversal was done for the same cases in the coarse-grained model for the sake of consistency. This also meant the ΔG_1 and ΔG_4 values for those simulations had to be multiplied by -1 as they had performed in reverse.

A

```
; residue  54 GLU rtp GLU  q -1.0
   446         N     54    GLU      N    170      -0.31    14.0067                                    ; qtot -0.31
   447         H     54    GLU      H    170       0.31     1.008                                     ; qtot 0
   448       CH1     54    GLU     CA    171          0    13.019                                     ; qtot 0
   449       CH2     54    GLU     CB    171          0    14.027  CH2      0.266     14.027          ; qtot 1
   450       CH2     54    GLU     CG    171          0    15.9994 OA       -0.674    15.9994         ; qtot 1
   451         C     54    GLU     CD    172       0.27    12.011  H        0.408     12.011          ; qtot 1.27
   452        OM     54    GLU    OE1    172     -0.635    15.9994 DUM      0.0       15.9994         ; qtot 0.635
   453        OM     54    GLU    OE2    172     -0.635    15.9994 DUM      0.0       15.9994         ; qtot 0
   454         C     54    GLU      C    173       0.45    12.011                                     ; qtot -0.55
   455         O     54    GLU      O    173      -0.45    15.9994                                    ; qtot -1
```

B

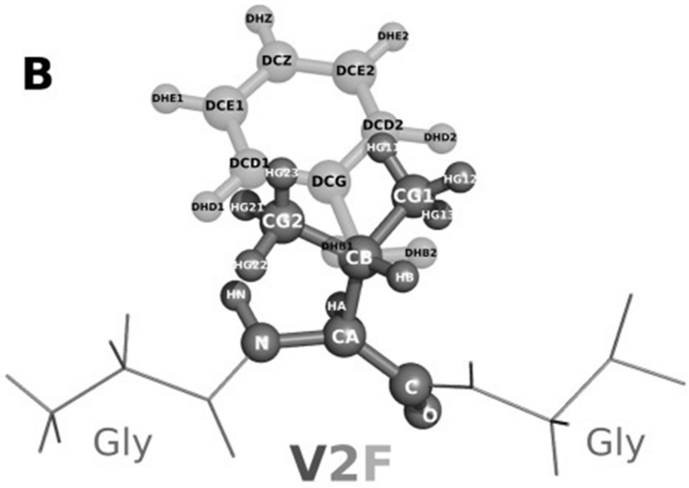

Figure 2: Hybrid topologies. **A:** Topology file of a S54E SNARE for the GROMOS force field, the hybrid residue is shown, the largest residue (here glutamate) being used as the first state. **B:** a visualization of the structure of a tripeptide with a V2F (Valine to phenyl alanine) hybrid residue. Valine (dark gray) is in the physical state A, whereas phenylalanine (light gray) is in the state B. If the larger residues was taken as state A less atoms would need to be added during manual editing of the topology files. (image retrieved from *Seeliger, D. & de Groot(2010)*[22])

For the Martini force field restrained bonds between beads involved in the TI were given as bond with a high force constant because otherwise TI cannot be performed. These force constants were rendered as two variants: fc_100000 and fc_1000000. This was done because the second version was advised by the Martini 3.0 force field as it was given in the topology file as the value to give for bonds replacing constraints if the molecule was set to flexible, but using this value required a smaller time step. Therefore fc_100000 was chosen and used until the force constant of a bond of the phosphorylated serine exceeded this value. Afterwards fc_1000000 were performed to investigate if it would produce significant difference in the results as the force constant of a non-restrained bond exceeding that of a restrained one would be highly unusual.

For the AMBER force field the online pmx server[36,37,47,48] was used to generate the hybrid structure. The topology files were edited so that for all particles the masses of both states were the same (if there was a second state), the mass being set to the highest mass of the two states. This is necessary because otherwise the simulations become numerically unstable. After these modifications the scripted preprocessing would be initiated. A slightly modified version of AMBER99sb-ILDN[25] (downloaded from the pmx website) was used which contained the topologies of the mutations.

For phosphorylated proteins and peptides the Vienna PTM 2.0 webserver[49–52] was used to generated the necessary pdb files for the GROMOS force field. A modified version of the GROMOS54a7 force field was used to accommodate for the new post-translationally modified residues. This force field was used for all simulations of the GROMOS force field, unmodified GROMOS54a7 was only used for the simulations of the mutations to alanine and glutamate using ALA-X-ALA tripeptides without a bigger box size, PME or shifting ions. Phosphorylation was not applied for the AMBER99sb-ILDN force field because no generator for post translational modifications for AMBER force field could be found that was compatible with GROMACS software[28,29]. For Martini force field the phosphorylated residues had to be manually parameterized(see below).

Thermodynamic integration

Thermodynamic integration(figure 3) was performed as described Seeliger and De Groot[22]. Thus $\Delta\Delta G = \Delta G_1 - \Delta G_4 = \Delta G_3 - \Delta G_2$ is used as an indicator of the differences in the free energy of folding between the two states. ΔG_1 is the free energy difference between mutant and Wild Type(WT) unfolded states, ΔG_2 is the free energy of folding of the mutant proteins while ΔG_3 is that of the WT protein and ΔG_4 is the free energy difference between mutant and wild type folded states. Thus the value of the $\Delta\Delta G$ indicates if the ΔG_2 or the ΔG_3 has a higher value (in the former case the $\Delta\Delta G$ will be positive in the latter case it will be negative). Either ALA-X-ALA or GLY-X-GLY tripeptides are used as reference for the unfolded state of the protein (X being the residues that are mutated or phosphorylated).

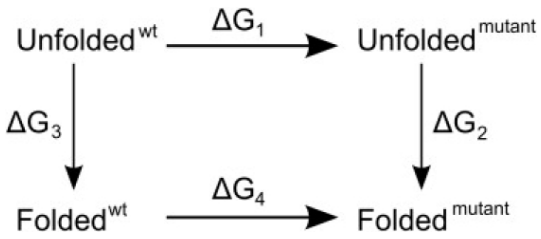

Figure 3: The Thermodynamic cycle. The unfolded state was modeled with capped AXA or GXG peptides (*X* = any amino acid). From the thermodynamic cycle, the folding free energy difference $\Delta\Delta G = \Delta G_3 - \Delta G_2$ between the wild-type protein and the mutant can be calculated via $\Delta G_1 - \Delta G_4$.(image retrieved from *Seeliger, D. & de Groot(2010)*[22])

The thermodynamic integration was run at a reference temperature of 310 K (normal body temperature) and reference pressure of 1 bar, v-rescale[53,54] temperature coupling and isotropic Berendsen[55] pressure coupling were used. For neighbor searching Verlet[56] cutoff schemes and grid searching were used. AMBER used Particle-Mesh Ewald (PME)[43] electrostatics GROMOS and Martini force fields initially used reaction field[42] but later PME was also used for better comparison with AMBER. Martini simulations using PME were run without polarizable water model. GROMOS and AMBER force fields used one femtosecond time step while Martini used 20 femtosecond time step (decreased to 10 fs for serine phosphorylations and to 5 fs for fc_1000000 simulations). The λ values used for the thermodynamic integration were: 0.0, 0.01, 0.1, 0.2, 0.4, 0.6, 0.8, 0.9, 0.99, 1.0.The details are in the run.mdp files in the supplementary data.

Simulations for GROMOS and AMBER were run for 10 ns while simulations for the Martini force field were run for 6.2 ns unless stated otherwise. Simulations for GROMOS and AMBER force fields were send to the Peregrine HPC cluster[21] to speed up the simulations.

In case of the AMBER force field an additional run was performed for both ALA-X-ALA and GLY-X-GLY tripeptides in which the masses of the beads changed along with the types. This could not be done for the SNAREs as that would result in numerical instabilities.

Simulations using shifting NAf ions (for topologies see supplementary data) were performed only for mutations to glutamate and for phosphorylation. One NAf ion was needed for the simulations of the mutations to glutamate to keep the net charge of the system the same for all λ points, two NAf ions were required to do the same for the phosphorylation simulations.

For the GROMOS and AMBER force fields the simulations of threonine to glutamate mutations (glutamate technically being the first state as it is the larger residue) had a tendency to become unstable at higher λ values. As a result it became necessary to split the threonine to glutamate mutation into two different steps: glutamate to serine and threonine to serine. With the AMBER force field T47E remained stable and was thus run normally and with the two-step process to see which effect the splitting of the simulation would have on the results.

Parameterization of Post translational modified residues

The parametrization was done according to the instruction on the Martini website for parameterizing molecules based on atomistic simulations[27].

The phosphorylated residues were mapped in the same manner as their unphosphorylated counterparts only adding a SD bead for the phosphate group (see supplementary figures 1a and b for details).

ALA-X-ALA tripeptides (X being either phosphorylated threonine(PTH) or phosphorylated serine(PSE)) were run using a Gromos54a7 force field with a reference temperature of 310 K and reference pressure of 1 bar, v-rescale[53,54] temperature coupling and isotropic Berendsen[55] pressure coupling were used. The time step was 1 femtosecond and the simulation length was 5 nanoseconds. For neighbor searching Verlet[56] cutoff schemes and grid searching were used.

An index file was created for both tripeptides in which the atoms were grouped in the same manner as they are mapped in the Martini force field. These index files were used to get the bond lengths and angles between the clustered groups. Then Martini topology files were made for the tripeptides and were run with settings as similar as possible to those of the atomistic simulation (time step was 20 femtoseconds until high force constant forced the time step be reduced to 10 femtoseconds). Several different values were tried out until significant overlap was achieved for bonds and angles between the atomistic simulation and the coarse-grained one (see supplementary files).

Mdp files used for simulations are included in supplementary files (run2-gromos.mdp for the GROMOS force field, run2-gromos-PME.mdp for the GROMOS force field using PME, run2-amber.mdp for the AMBER force field, run2-martini.mdp for Martini force field, run2-martini-PME.mdp for Martini force field using PME).

Results and discussion

Simulation were run for mutations to alanine and to glutamate for all three force fields (GROMOS, AMBER and Martini). In addition for the GROMOS and Martini force fields phosphorylation was simulated as well, because in vivo phosphorylation of the residues is what stalls the SNARE mediated membrane fusion[7]. Phosphorylation was not performed for the AMBER force field due to lack topologies of phosphorylated residues compatible with GROMACS[28,29]. All simulation types were performed with both ALA-X-ALA and GLY-X-GLY tripeptides for the unfolded state. ALA-X-ALA tripeptides were used because in Martini 2.2 using GLY-X-GLY would give the wrong backbone bead[57,58]. The GLY-X-GLY were used because those tripeptides were advised by Seeliger en de Groot[22], but it was also done to see if using ALA-X-ALA tripeptides instead of GLY-X-GLY would give significantly different results.

The AMBER simulations where beads shift mass were initially done to generate ΔG_1 values that could be compared with those given on the pmx website[37] in the tripeptide database which use changing mass by default. It was however also done in order to compare them to the values without shifting mass. Thanks to the numerical instabilities in the simulations of the SNARE complex using shifting mass beads the ΔΔG had to be calculated using SNAREs without shifting masses instead. However as a result the changes between state A and B are not exactly the same for the SNAREs as for the tripeptides under these conditions, which may mean that the resulting ΔΔGs are less reliable and accurate. The resulting ΔΔGs were still calculated to see if the use of shifting mass tripeptides in combination with SNARE without shifting mass would result significant difference with the ΔΔGs of when both tripeptides and SNAREs do not shift masses. That way the reliability of shifting mass tripeptides in combination with SNAREs that do not shift mass could be tested.

In case of the GROMOS force field the variant used for the post-translationally modified proteins and tripeptides was also used for the unphosphorylated proteins and tripeptides to allow for better comparison. This was also done because the unmodified version of GROMOS54a7 used dihedral type 39 for a dihedral involving the N-terminal NH_3 group which is not the correct type as that should be dihedral type 29[24]. Since the modified version of the force field was more correct the unmodified version was not used after the first set of simulations (unmodified ALA-X-ALA simulations for mutations to alanine and glutamate).

In the initial simulations of both mutations to alanine and to glutamate as well as in those of phosphorylation there could be large differences (often ~10 KJ/mol for mutation to alanine and often ≥20 KJ/mol for the rest) between the force fields even between the two atomistic force fields. In order to resolve the difference between the force field several different conditions for the simulation were tried. Martini 3.0.4[23] is a coarse-grained force field and thus has a lower amount of details in comparison to the atomistic force fields which might cause larger differences with either of the atomistic force fields[26], thus making large differences less unexpected. Also Martini 3.0.4 is still being tested and thus could still have some errors.

An examination of initial simulations revealed the SNARE would pass to the periodic boundaries of the box during the simulations, which can cause the SNARE to interact with itself through these periodic boundaries. When using a dodecahedron instead of a triclinic box the box size would increase and the SNARE would no longer pass through the periodic boundaries. Thus this increased box size was used for the simulations for the GROMOS and AMBER force fields to reduce the differences between the force fields. Due to a quirk in the preprocessing the Martini force field used this bigger box size from the start.

The GROMOS and Martini force fields used reaction field electrostatics during the initial simulations while the AMBER force field used PME electrostatics. This difference could possibly be the reason for the difference in ΔΔG between the different force fields, thus the GROMOS and Martini force fields simulations were also performed using PME to see if this was truly the case.

For the Martini 3.0.4 force field the PME simulations were run without polarizable water model. There is a polarizable water model for one of the previous versions of Martini[59] but not yet for Martini3[23] and there have been a lot of changes between the first Martini force[26] field and Martini 3.0.4[23]. Therefore using the polarizable water model of an older version of the Martini force field might not work properly for the Martini 3.0.4 force field. Not using polarizable water was also done to see what the use of PME without polarizable water model would result in for the Martini 3.0.4 force field.

As the TE, SE, TpT and SpS hybrid residues shift in state, the charges will change as well resulting in a larger charge for the system, which may alter the value of ΔΔGs and is not representative of the situation in vivo. Thus simulations in which the net charge would remained the same over all λ points were performed for the

mutations to glutamate and phosphorylation. In order to do this some NA^+ ions were replaced by NAf ions(see supplementary files) which are NA^+ ions who have a second state where the charge is zero, thus causing the net charge of the system to remain the same.

All possible combinations between these three alterations to the conditions were tried as well to see if a combination of those conditions could reduce the difference between the force fields in case one of those conditions alone was not enough.

A more detailed description of the results of the mutations to glutamate and the phosphorylation is included in the supplementary data.

Mutating the key residues to alanine had a stabilizing effect on the SNARE complex

According to Malmersjö *et al.*[7] mutations of residues 47, 53, 54 and/or 61 to alanine would improve membrane fusion. Here(figure 4, figure S1) mutating these residues to alanine generally resulted in a positive ΔΔG which indicates that the mutation decreased the free energy of folding and thus making folding more favorable, supporting the conclusion by Malmersjö et al. It must however be noted that in all cases, except those of the GROMOS force field using PME and a bigger box size and the Martini 3.0 force field (both higher and lower force constant), mutating residue 47 to alanine resulted in a negative ΔΔG. In case of the AMBER force field the ΔΔG of the T53A mutation is also negative. These values remained negative even when using a bigger box size and/or PME.

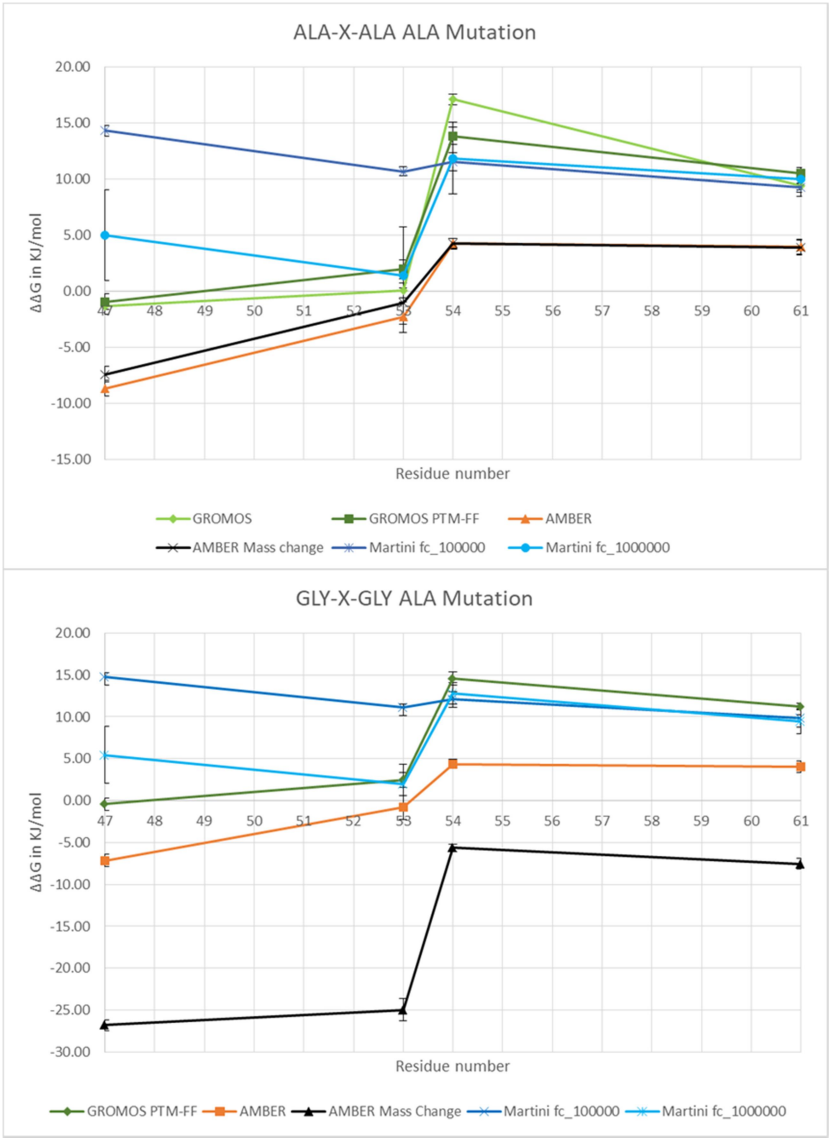

Figure 4: Mutations to alanine presented in a scatterplot graph. On the x-axis is the residue number of the residue being mutated, on the y-axis is the ΔΔG given in kJ/mol. GROMOS force field values are given in green, AMBER in orange and Martini in Blue. Given in black are the values for the AMBER force field calculated using tripeptides that shift mass, which may have reduced reliability. **Top:** the ΔΔGs of the simulations using ALA-X-ALA as the unfolded state, not using a bigger box size or PME. Graph indicated as simply GROMOS (given in light green) refers to values calculated using the force field without post translational modification. **Bottom:** the ΔΔGs of the simulations using GLY-X-GLY as the unfolded state, not using a bigger box size or PME.

In the fc_100000 results of the Martini force field the ΔΔG of T47A has a higher value than that of T53A which in turn has a lower ΔΔG than S54A, S54A has higher ΔΔG than S61A. In case of the GROMOS and AMBER force fields the ΔΔG of T47A is lower than that of T53A but otherwise the pattern is the same as with Martini fc_100000. The Martini fc_1000000 results look like they have the same pattern as the fc_100000 counterpart however there is a relatively large standard deviation(~3.0 kJ/mol vs <2.0 kJ/mol for all other conditions)(figure S1) around the T47A, T53A and S54A; which means that it might also have the same pattern as the GROMOS and AMBER force fields. The larger standard deviation is likely due to the fact that the phase space has been less extensively sampled as the higher force constant means slows down movement of the bonds and thus sampling. Overall the average values the Martini fc_1000000 has for T47A and T53A better match those of an atomistic force field (specifically GROMOS) than the fc_100000 variant whose values for those residues are close to neither GROMOS or AMBER. This indicates that the fc_1000000 variant is most likely more accurate than the fc_100000 variant, especially under the PME with a bigger box size conditions where the differences between the two force fields are within 2.5 kJ/mol for all residues.

Increasing the box size by making the box a dodecahedron(figure S1) did slightly alter the ΔΔG and the standard deviation but the values remained close(within ~2.5 kJ/mol) to the values of the smaller box and the patterns did not change. The same holds true for the use of PME (figure S1) and for the combination of a bigger box size and PME (figure S1). This indicates that the smaller box size or use of reaction field did not severely affect the outcomes of the simulations of the ALA mutations. This likely due to the fact the charges do not change for the mutations to alanine, as increasing the box size does have a significant effect on mutations to glutamate and the phosphorylation(see below).

To check the quality of the AMBER simulations, the GLY-X-GLY mass change data were compared to the values of the pmx website[47]. For the threonine to alanine mutations that was 120.98 ± 0.27 kJ/mol on the pmx website vs 113.19 ± 0.27 kJ/mol from the simulations. For the serine to alanine mutations that was 39.09 ± 0.19 kJ/mol on the pmx website vs 46.56 ± 0.30 kJ/mol from the simulations. The difference between the simulations and the data on the website is ~ 7 kJ/mol which seems to be within reasonable bounds and can be explained by differences in the run settings, as larger differences have been found within the simulations performed here as a result of different settings. This means that the AMBER simulations are likely to have decent quality for the mutations to alanine. This comparison could not be performed for the mutations to glutamate or for phosphorylation as there was no data available for those mutations on the pmx website.

In case of the ΔΔG calculated using GLY-X-GLY with mass change for the AMBER force field resulted in negative ΔΔG's for all four residues for both the smaller and the large box size variants. This likely means that the mass change AMBER variant is the least accurate simulation as these results are the only ones showing this tendency. This does give confirmation that tripeptides that change mass in combination with SNAREs that don't have reduced reliability and accuracy.

Aside from the situation with mass change for the AMBER force field all statements made for ALA-X-ALA also hold true for GLY-X-GLY. In fact, with exception of again mass change for the AMBER force field, the average values of and standard deviation of the ΔΔGs of GLY-X-GLY differ less than 1 kJ/mol from their ALA-X-ALA counterpart.

With the exception of the Martini fc_1000000 without PME all none of the standard deviations are capable of shifting to relative position of ΔΔGs thus disrupting the pattern of relative effect. Therefore the mutations to alanine the patterns do not need to be doubted especially those where PME is used.

The differences between the ΔΔG between the GROMOS and AMBER force fields is ~5-10 kJ/mol and none of the alterations that were tried (bigger box size and use of PME) resolved those differences for either ALA-X-ALA or GLY-X-GLY tripeptides. The exact differences between the different residues could noticeably be altered by the different conditions but the pattern of relative effects could not.

Mutating the key residues to glutamate had a destabilizing effect on the SNARE complex

According to Malmersjö *et al.*[7] mutations of residues 47, 53, 54 and/or 61 to alanine would inhibit membrane fusion. Here(figure 5, figure S2, figure S3) mutating these residues to glutamate generally resulted in a negative ΔΔG which indicates that the mutation increased the free energy of folding and thus making folding more unfavorable.

In almost all cases the ΔΔG of T47E was lower than that of T53E which is higher than that of S54E, the ΔΔG of S54E is lower than that of S61E. The exception to this rule being fc_1000000 simulations where T53E has a lower value than S54E but the rest of the pattern is the same. T47E had a more negative ΔΔG than S54E for the

AMBER force field unless the combination of a bigger box size and shifting ions(figure 5, figure S3) are used, in which case the opposite is true. For the GROMOS force field T47E had a more negative ΔΔG than S54E when shifting ions without a bigger box size are used(figure S3), but a less negative ΔΔG under all other conditions.

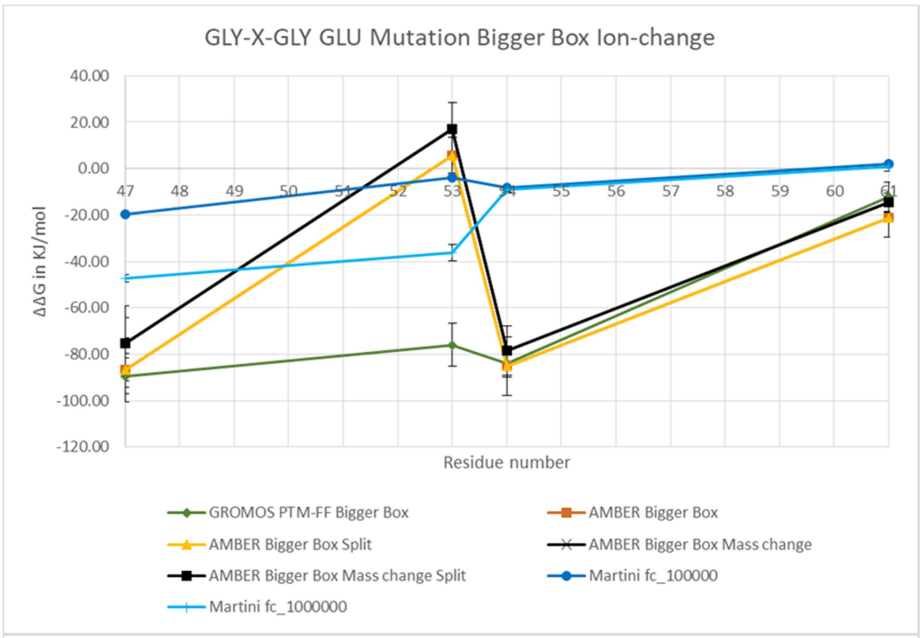
GLY-X-GLY GLU Mutation Bigger Box Ion-change
40.00
20.00
0.00
-20.00
-40.00
-60.00
-80.00
-100.00
-120.00
47 48 49 50 51 52 53 54 55 56 57 58 59 60 61
ΔΔG in KJ/mol
Residue number
GROMOS PTM-FF Bigger Box
AMBER Bigger Box
AMBER Bigger Box Split
AMBER Bigger Box Mass change
AMBER Bigger Box Mass change Split
Martini fc_100000
Martini fc_1000000

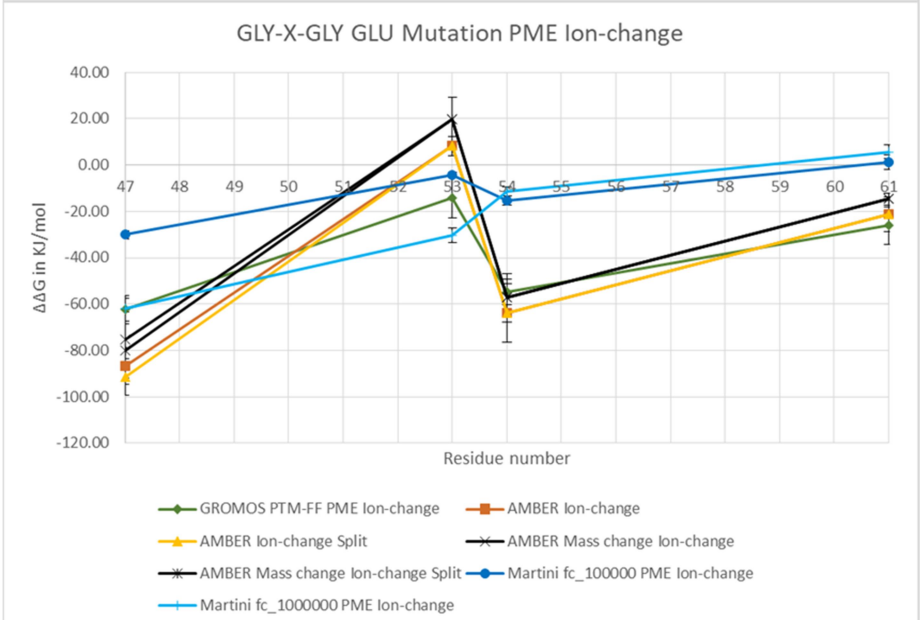
GLY-X-GLY GLU Mutation PME Ion-change
40.00
20.00
0.00
-20.00
-40.00
-60.00
-80.00
-100.00
-120.00
47 48 49 50 51 52 53 54 55 56 57 58 59 60 61
ΔΔG in KJ/mol
Residue number
GROMOS PTM-FF PME Ion-change
AMBER Ion-change
AMBER Ion-change Split
AMBER Mass change Ion-change
AMBER Mass change Ion-change Split
Martini fc_100000 PME Ion-change
Martini fc_1000000 PME Ion-change

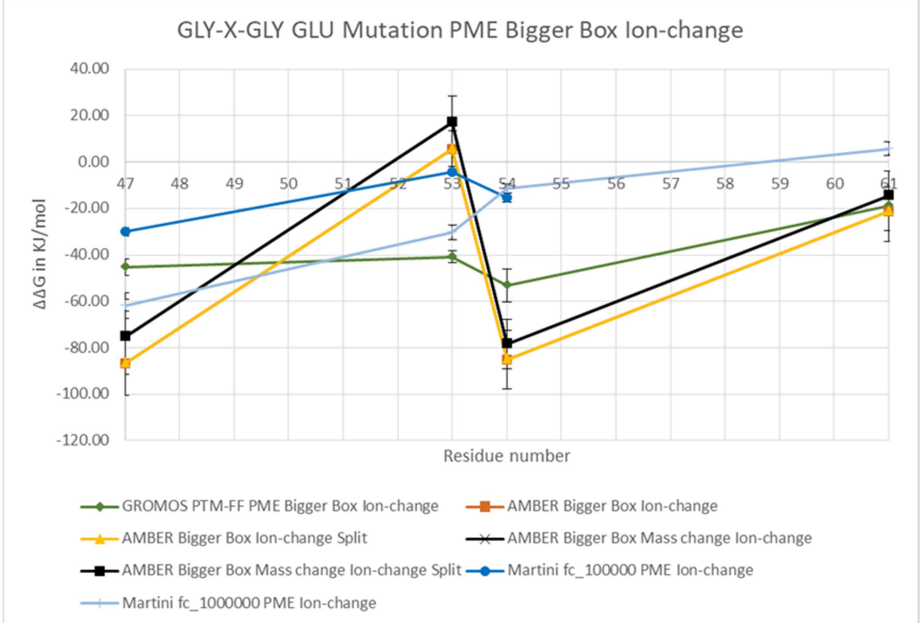
GLY-X-GLY GLU Mutation PME Bigger Box Ion-change
40.00
20.00
0.00
-20.00
-40.00
-60.00
-80.00
-100.00
-120.00
47 48 49 50 51 52 53 54 55 56 57 58 59 60 61
ΔΔG in KJ/mol
Residue number
GROMOS PTM-FF PME Bigger Box Ion-change
AMBER Bigger Box Ion-change
AMBER Bigger Box Ion-change Split
AMBER Bigger Box Mass change Ion-change
AMBER Bigger Box Mass change Ion-change Split
Martini fc_100000 PME Ion-change
Martini fc_1000000 PME Ion-change

Figure 5: Mutations to glutamate presented in a scatterplot graph. On the x-axis is the residue number of the residue being mutated, on the y-axis is the ΔΔG given in kJ/mol. GROMOS force field values are given in green, AMBER in orange and Martini in Blue. Given in black are the values for the AMBER force field calculated using tripeptides that shift mass, which may have reduced reliability. **Top:** the ΔΔGs of the simulations using GLY-X-GLY as the unfolded state, using a bigger box size and shifting ions. **Middle:** the ΔΔGs of the simulations using GLY-X-GLY as the unfolded state, using PME and shifting ions. **Bottom:** the ΔΔGs of the simulations using GLY-X-GLY as the unfolded state, using a bigger box size, PME and shifting ions.

In the Martini fc_1000000 simulations the T47E and T53E mutations had at first instance large standard deviations (~30-40 kJ/mol), those turned out to be caused by the fact that the chosen length for the equilibration run had been too short for this type of mutation in the Martini force field as both tripeptides as SNAREs fluctuated heavily in the first ~1000-2000 ps. Cutting the first 2000 ps off solved this issue and significantly reduced the standard deviation to be ≤ 5.41 kJ/mol.

In general the difference in ΔΔG between GROMOS and AMBER can be as much as 30 kJ/mol. These are significant amounts that should normally not occur. There is an even bigger difference between either these force fields and the Martini force field, as the Martini force field has ΔΔGs which are less negative than those for GROMOS and AMBER especially when the lower force constant is used.

Increasing the box size (figure S2) did significantly alter the values of the ΔΔG and the standard deviation. This reduced total difference in ΔΔG between the AMBER and GROMOS force fields, this effect was similar but less strong for GLY-X-GLY. The usage of PME (figure S2) for GROMOS and Martini force fields did significantly alter the values for GROMOS and Martini fc_1000000 (not for AMBER as AMBER can only use PME electrostatics). GROMOS is affected in a similar manner as when the box size is increased. However instead of the differences between the GROMOS and AMBER force fields becoming smaller they became bigger. When using both a bigger box size and PME (figure S2) the differences between the GROMOS and AMBER force fields are bigger than when only the bigger box size is used, but smaller than for conditions without alterations or when only PME is used.

When using ions that shift state overall the differences between the AMBER and GROMOS force fields became bigger in comparison to the unaltered conditions. In fact the differences became bigger than with all previously tried conditions. Remarkably T53E became strongly positive for the AMBER force field and remained so for all combination involving shifting ions. No explanation for this behavior could be found but cutting of the first 2 ns of the simulations(figure S7) did not give a negative ΔΔG. Therefore improper equilibration has been ruled out as the cause of the strongly positive ΔΔGs.

When combining shifting ions and a bigger box size(figure 5, figure S3) the differences between the GROMOS and AMBER are overall not smaller nor bigger for either ALA-X-ALA nor GLY-X-GLY in comparison to when only shifting ions are used. It must be noted however that the ΔΔGs of GLY-X-GLY are much smaller for all residues except for T53E.

For GROMOS combining the use shifting ions and PME(figure 5, figure S3) brings for ALA-X-ALA the all ΔΔGs (with the exception of T53E which has a much larger difference) of the GROMOS force field were within ~5-8 kJ/mol of the (not-split) AMBER force field simulation. The combination of shifting ions, a bigger box size and PME(figure 5, figure S3) has differences between the GROMOS and AMBER force fields that are (with the exceptions of S61E) 20 kJ/mol or larger than those of only shifting ions. Overall this makes the differences not only larger than those of both only using shifting ions and PME, but also those of only shifting ions and a bigger box size, giving the largest difference yet found. This means that using shifting ions and PME gave best match between the GROMOS and AMBER force fields for ALA-X-ALA, indicating these conditions might be the best ones for the mutations to glutamate. With GLY-X-GLY there are some differences; with the combination of PME and shifting ions T47E has a larger difference while that of T53E is smaller and for S54E and S61E the

differences are more or less the same for both ALA-X-ALA and GLY-X-GLY. These values mean however that the overall difference are more or less the same. The statements made with ALA-X-ALA about the combination of shifting ions, a bigger box size and PME also hold true for GLY-X-GLY. Like ALA-X-ALA shifting ions and PME gave a very good match between GROMOS and AMBER unlike ALA-X-ALA the combination of a bigger box size and shifting ions is another promising candidate. For GLY-X-GLY the differences of bigger box size and shifting ions in comparison to PME and shifting ions are much smaller for 3 of the 4 key residues but significantly larger for the fourth one (T53E). This indicates the discrepancies between the force fields was likely an effect of the changes in as PME and shifting ions primarily work on the electrostatics.

For the Martini force field there is no shift larger than ~8 kJ/mol except when PME and shifting ions are combined. Overall the shifts in the Martini force field do not contribute as significantly towards a reduction of the difference with either the GROMOS or the Martini force fields, as the shifts of the other force fields do. The differences with the GROMOS force field are the smallest when using PME and shifting ions. The differences with the AMBER force field are the smallest when only a bigger box size is used although the combination of PME and shifting ions was a close runner up for GLY-X-GLY, as except for T53E all differences there were smaller than when only a bigger box size was used.

The standard deviations are typically within or close to 2.5 kJ/mol for GROMOS and Martini and around the 5-8 kJ/mol) for AMBER(figure S2). The standard deviations when using shifting ions are around the 6 kJ/mol for GROMOS , 10 kJ/mol for AMBER and within 2.5 kJ/mol of for the Martini force field figure S3), it must be noted however that for GROMOS and AMBER standard deviations as high as 15 kJ/mol could be reached. Despite the sometimes large values the standard deviations are not capable of disrupting the pattern of relative effects except between T47 and S54 for the AMBER and T47 and T53 for GROMOS, which had values that were close to each other relative to those of the other residues.

Using ions that shift state had some interesting effects on the simulations of both the mutations to glutamate and of phosphorylation. First to note is for the AMBER and GROMOS force fields both the ΔG_1 and ΔG_4 became ~1.5-2.0 as big as before. Also there was a strong increase in the standard deviation for the GROMOS force field especially in case of the phosphorylation simulations. In all likelihood the fact that more beads shift charges causes the system to fluctuate more which increases the standard deviations. However the charges that appear or disappear when the residues shift state are balanced out by the shift in charge of the ionic beads. Thus using ions that shift state has both advantages and disadvantages. In a future project it should be looked into if any additional settings make the usage of ions that shift state more efficient and/or accurate.

Splitting the TI into two parts did significantly affect the final values (difference ~20 kJ/mol). Which means that splitting up the simulation can cause some unreliability in the results. On the other hand, the combination of ions that shift state and a bigger box size reduces the differences between the averages values to be smaller than 0.5 kJ/mol, but the standard deviation under those conditions can be rather large so this needs to be interpreted with caution.

Phosphorylating the key residues had a destabilizing effect on the SNARE complex with a varying pattern of relative effects

The phosphorylation is particularly interesting to look at as it is typically transient making the effects it has on free energy of folding difficult to measure. This why Malmersjö *et al.*[7] decided to use mutation to glutamate to mimic the effects of phosphorylation on the SNAREs. Here(figure 6, figure S4) it is possible to simulate phosphorylation directly and thus observe its results. The ΔΔGs of this study are almost all negative indicating that the phosphorylation increased the free energy of folding and destabilizing the SNARE.

For the GROMOS simulations, increasing the box size(figure 6, figure S4) did significantly alter the ΔΔG, especially in the case of S54pS which became ~50 kJ/mol more negative. Because the other ΔΔGs became ~20-30 kJ/mol less negative than those of the smaller box, the shift of S54pS altered the pattern of the relative effects of the residues. The resulting pattern matches that of mutations to glutamate. This holds true for both ALA-X-ALA and GLY-X-GLY(figure S4).

Figure 6: Phosphorylation presented in a scatterplot graph. On the x-axis is the residue number of the residue being mutated, on the y-axis is the ΔΔG given in kJ/mol. GROMOS force field values are given in green and Martini in Blue. **Top left:** the ΔΔGs of the simulations using ALA-X-ALA as the unfolded state, both with and without the use of a bigger box size. **Top right:** the ΔΔGs of the simulations using ALA-X-ALA as the unfolded state, using PME both with and without the use of a bigger box size. **Bottom left :** the ΔΔGs of the simulations using ALA-X-ALA as the unfolded state, using shifting ions both with and without the use of a bigger box size. **Bottom right:** the ΔΔGs of the simulations using ALA-X-ALA as the unfolded state, using PME and shifting ions both with and without the use of a bigger box size.

In contrast to the mutations to GLU and ALA the Martini fc_100000 and fc_1000000 have the same pattern of relative effects and have very similar values (with the exception of T53E they are all within 2.5 kJ/mol of each other) in case of the ALA-X-ALA simulations. The pattern of relative effects are however different when comparing the different force constant variants for GLY-X-GLY(figure S4). In case of the fc_100000 the T47pT and T53pT both have a higher ΔΔG than S54pS, while in case of the fc_1000000 both have a lower ΔΔG. The values of S54pS and S61pS have a difference smaller than 2.5 kJ/mol between the fc_100000 and fc_1000000 variants. S61pS has a slightly positive ΔΔG.

For the GROMOS simulations using PME(figure 6, figure S4) altered the pattern of relative effects again as T53pT now has a more negative ΔΔG than T47E while S61pS now has a less negative ΔΔG than S54pS. This is the opposite of what is the case under conditions without alterations. When a bigger box size and PME were used a pattern of relative effects matching that of the mutations to glutamate would be found, just like when only a bigger box size is used.

For Martini fc_100000 and fc_1000000 using PME(figure 6, figure S4) did not alter the patterns of expression already present for both ALA-X-ALA and GLY-X-GLY. In addition the values of the Martini force field did not get any closer to those of GROMOS. The differences between the ΔΔGs of fc_100000 and fc_1000000 also remained more or less the same, with the differences being within 5 kJ/mol of their values without PME.

For the GROMOS simulations using shifting ions(figure 6, figure S4) altered the pattern of relative expression as S54pS became more negative than T53pT yielding a pattern that is similar to that of mutations to glutamate.
Increasing the box size in addition to using shifting ions(figure6, figure S4) makes S54pS positive at a value of 17.91 kJ/mol for ALA-X-ALA and 48.34 for GLY-X-GLY(figure S4). It must be noted however that S54pS has a standard deviation of 23.08 kJ/mol for ALA-X-ALA which can put the ΔΔG in the negatives, The standard deviation of GLY-X-GLY (27.29 kJ/mol) is however not enough to do this. These large standard deviations also mean the results may be less reliable. But this positive value is unusual as phosphorylation has a destabilizing effect and should thus give a negative ΔΔG. The pattern of relative effects was also altered as prior to increasing the box size. S54pS had a less negative value than T53pT while after the box size increased the roles were reversed. Most peculiarly the resulting pattern no longer has symmetry with the mutations to glutamate. This is the opposite of the previous situations where there was symmetry with the mutations to glutamate when a bigger box size was used but not when a smaller one was used.
When using PME in combination with shifting ions S61pS became strongly positive at a value of 43.87 for ALA-X-ALA and 24.66 for GLY-X-GLY. The standard deviation of S61pS (16.93 for ALA-X-ALA, 15.52 for GLY-X-GLY) is not enough to place the ΔΔG within the negatives, unlike S54pS when a bigger box size and shifting ions are used. The pattern of relative effects alters again in comparison to when only shifting ions are used, now resembling the pattern found for mutations to glutamate.
Using a bigger box size and PME and shifting ions will make the ΔΔG S61pS close to 0 kJ/mol. The standard deviation of S61pS remains more or less the same, which means that the ΔΔG can end up in the negative values. The pattern of relative effects remained the same as prior to increasing the box size, meaning that for phosphorylation the pattern of relative effects will only stop changing when both PME and shifting ions are used.

For GLY-X-GLY(figure S4) the pattern of relative effect is the same as with ALA-X-ALA under all possible conditions even if the exact values can differ by as much as 30 kJ/mol. This means that for the phosphorylation in the GROMOS force field which tripeptides are used for the unfolded state can have an effect on the exact values of the ΔΔGs but not on the pattern of relative effects.

When using shifting ions the ΔΔGs of Martini fc_100000 T53pT of GLY-X-GLY(figure S4) became strongly positive at a value of 16.17, for ALA-X-ALA the shift is less strong with the value ending up at 2.19 kJ/mol. Unlike with similar situations in the GROMOS force field the standard deviation is 2.45 kJ/mol instead of larger than 10 kJ/mol. For both ALA-X-ALA and GLY-X-GLY the patterns of relative expression are the same as under conditions without alterations. The difference in ΔΔG values between GROMOS and Martini are overall not smaller than under conditions without shifting ions.

When using PME and shifting ions for the Martini force field the differences between the pattern of relative effects did not alter but the difference with the values of the GROMOS force field became smaller especially for the ALA-X-ALA fc_1000000 variant. For the fc_1000000 variant of ALA-X-ALA the ΔΔGs are with the exception of S54pS all within 8 kJ/mol of their counterparts in GROMOS with a bigger box size, PME and shifting ions. In case of T53pT and S61pS the difference are even within or close to 2.5 kJ/mol. While again with the exceptions of S54pS this even lower with fc_100000 that is only the case with ALA-X-ALA. For GLY-X-

GLY the differences are significantly larger than for ALA-X-ALA. Thus with GLY-X-GLY the fc_1000000 is still closer to acceptable bounds with the GROMOS force field than fc_100000. Thus the combination of bigger box, size PME and shifting ions overall seems to be the best match obtained for the phosphorylation mutations between the GROMOS and Martini force fields.

Despite mutations to glutamate and phosphorylation having the same pattern (when it stops shifting) differences between the two different mutation types can be as large as 20 kJ/mol or larger still. Considering that phosphorylation gives a divalent charge in comparison to the single charge of mutations to glutamate, a more negative ΔΔG for phosphorylation would be expected, this is not however always the case. Without shifting ions the mutations to glutamate most often give a more negative ΔΔGs than phosphorylation does or the values are overall more or less the same. When shifting ions are used for ALA-X-ALA then the phosphorylation does give more negative ΔΔGs than mutations to glutamate but this no longer the case if in addition to shifting ions also PME and/or a bigger box size are used. For GLY-X-GLY the use of shifting ions gives more negative ΔΔGs than mutations to glutamate even when PME or PME and a bigger box size is used, it is however not the case when only shifting ions and a bigger box size are used. It is wise to investigate this further in the future especially to see if phosphorylation does indeed have a stronger effect at suppressing vesicle fusion than mutations to glutamate in vivo.

With both Martini fc_100000 and fc_1000000 the ΔΔG of S61 is positive for the phosphorylation simulations and for the simulations of the mutations to glutamate when shifting ions are used. S61 has noticeably positive values of 5 kJ/mol or more for the fc_1000000 simulations of mutations to glutamate using PME and shifting ions and phosphorylation using shifting ions both with and without PME. All other values were within or close to 2.5 kJ/mol of zero. These occurrences are likely caused by the fact that in the simulated part of the SNAREs S61 was close to the C-terminus and was thus more in contact with the solvent and ions than the other residues which are further away from the termini. The increased contact with solvent and ions could in part compensate for the appearance of an additional charge thus making the ΔΔG positive. The fact the ΔΔG of S61 reaches more significantly positive values when shifting ions are used indicates this as the appearing positive charges of NAf would compensate for the appearing negative charges of glutamate and phosphorylated serine. The fact that this does not occur for the atomistic force fields is most likely caused by the difference of atomistic vs coarse-grained force fields and that Martini 3.0.4 is still being tested.

S54pS has very strong shifts for the GROMOS force field when the conditions change. This can be explained by the fact that the divalent charge of the phosphorylate residue has a very strong effect. This is very probable considering S54 has overall one of the strongest effects on the stability of the SNARE. Utilizing PME can strongly reduce these shift indicating that these shifts were indeed the results of the divalent charge influencing electrostatics.

The positive ΔΔGs for S54pS for shifting ions with bigger box size and S61pS for shifting ions with PME for the GROMOS force field are unexpected, as a phosphorylation in all other instances gives negative ΔΔGs. Even harder to explain is the positive value of T53pT for the GLY-X-GLY variant of Martini fc_100000 when only shifting ions were used, as unlike for the GROMOS force field there was no large standard deviation. No explanation for these discrepancies could be found but cutting of the first 2 ns of the simulations(figure S7) did not give a negative ΔΔG even if it did reduce the standard deviation by as much as 10 kJ/mol or more. Therefore improper equilibration has been ruled out as the cause of the strongly positive ΔΔGs. Cutting of the first 2 ns might also have reduced the standard deviation by cutting of a valley in the phase.

The standard deviations are around ~5 kJ/mol (± 2.5 kJ/mol) for both GROMOS and Martini force field(figure S4), except for Martini fc_100000 without PME where the standard deviations are smaller than 2.5 kJ/mol. The standard deviations when using shifting ions are typically around the 10-15 (sometimes as high as 20) kJ/mol for GROMOS. These standard deviations could not disrupt the pattern of relative effects under the conditions where the pattern is stabilized (PME and shifting ions), the exception being between T47 and T53 whose values were very close to one another (within 2.5 kJ/mol). Under the other conditions the pattern was more readily disrupted by the standard deviations. For the Martini force field the standard deviations are within or close to 2.5 kJ/mol when shifting ions are used but not PME, when both shifting ions and PME are used the standard deviations are around the 5 kJ/mol for threonine phosphorylation but within 2.5 kJ/mol for serine phosphorylation.

Due to the absence of AMBER there is less data available for the simulation of phosphorylation. This makes it more difficult to estimate the quality and success of the simulations performed for phosphorylation.

Martini-pmx can successfully make a hybrid topology for the Martini 3.0.4 force field

Pmx generates a hybrid topology in 3 steps: 1, use *mutate.py* to alter any number of residues in the pdb file into hybrid residues; 2, use *gmx pdb2gmx* of the GROMACS software to transform the pdb into a .top topology file and 3, use *generate_hybrid_topology.py* to add the second states for the atoms, bond, angles, dihedrals etc. to the topology file(s). The choice to adapt pmx for use of the Martini force field was made because the alternative was to make an entirely new program. That option would cost more time and might have ended with retracing the steps made by pmx.

Normally the force field called by *generate_hybrid_topology.py* needs to be the same as the one called by *mutate.py* for the pmx software to work[60]. However generating a topology file for the Martini3 force field requires usage of *martinize2* which combines the atoms into larger beads, instead of *gmx pdb2gmx* which cannot do this for larger atoms. *martinize2* can be used to make a martini topology which contains a hybrid residue with the first states as long as it recognizes the hybrid residue in the pdb. This means that the martini3 force field only needs to be expanded so that the hybrid residues in the altered pdb can be recognized by *martinize2* and inserted as the right residue in the topology. Therefore only the *generate_hybrid_topology.py* needs to be altered.

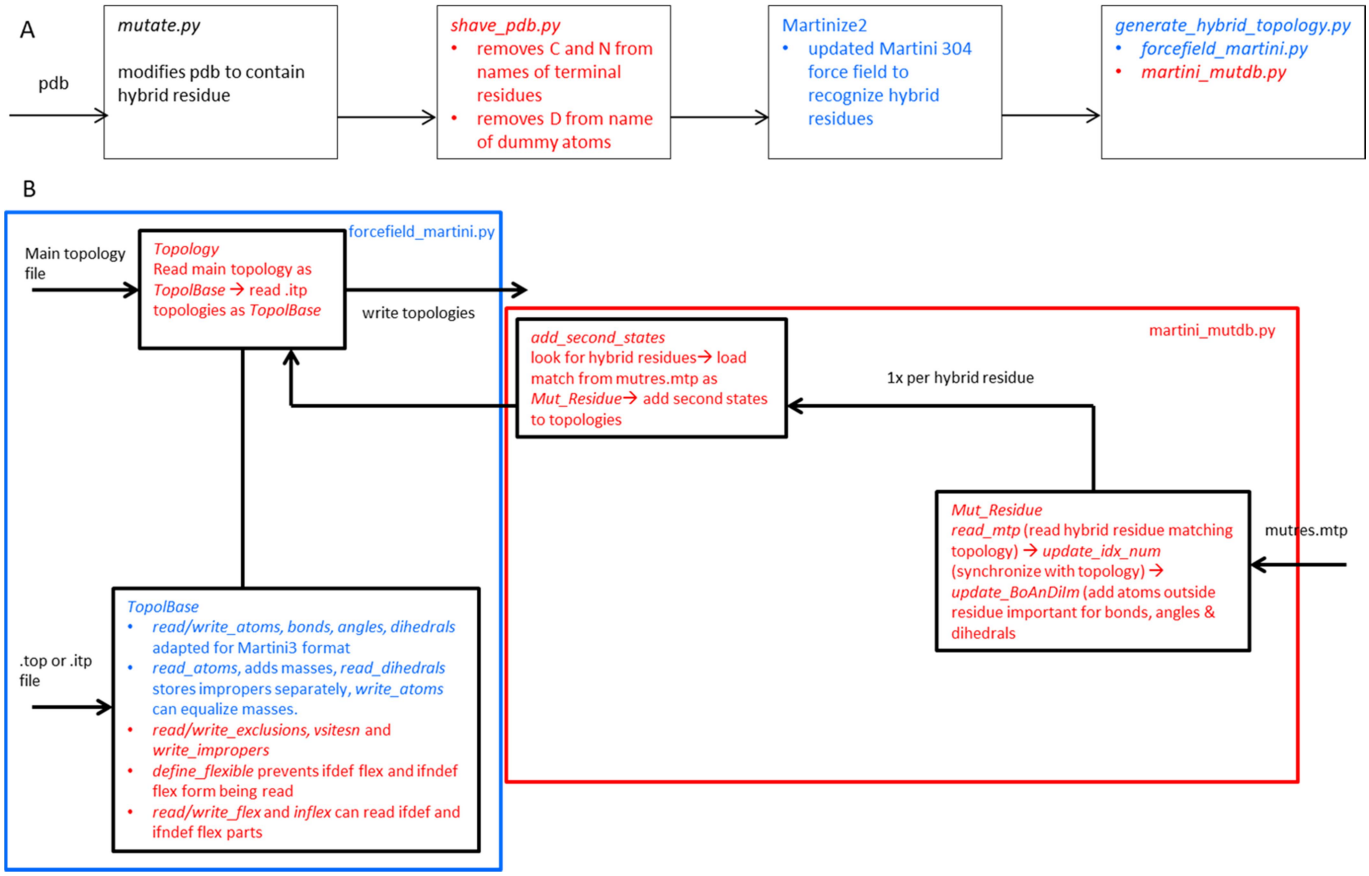

Figure 7: overview of the workflow and new components of martini-pmx. Scripts, functions and classes given in blue are a modified version of something that was present in the original pmx version, Scripts, functions and classes given in red are new for martini-pmx. **A:** Flowchart of the general workflow of martini-pmx. **B:** Flowchart visualizing the structure of how *generate_hybrid_topology.py* works for the Martini 3.0.4 force field.

generate_hybrid_topology.py(figure 7B) uses several functions which would not work for the Martini3 force field, such as the function *find_bonded_entries* which finds the length and force-constant for a implicitly defined bond. This would not work for Martini3 as in Martini force fields all bonds need to be explicitly defined[26]. There it seemed prudent to simply copy the classes and functions that were needed for the martini3 force field and alter them, adding any additionally necessary functions. Using this approach two new scrips were written *forcefield_martini.py* strongly based on *forcefield2.py* and *martini_mutdb.py* based on *mutdb.py* but also copying some functions from *generate_hybrid_topology.py*.

forcefield_martini.py contains two classes for handling topology files *TopolBase* and *Topology*. The TopolBase class was copied from the from *forcefield2.py* and subsequently altered. The some of the read and write functions that were already present were altered to utilize the format used by Martini3. The function to read the atoms (atoms being stored in a modified version Atom class as defined in standard pmx) was further altered to add the mass if it is not explicitly given (Martini topologies do not have to explicitly give the masses of the particles)[26] bases on the name/size of the particle because the masses need to explicitly given if a second state of an atom needs to be added. The function to read dihedrals was altered to store dihedrals with function type 2 (improper dihedrals)[26] under a separate list to make it easier to keep track of everything as improper/type 2 dihedrals don't have a multiplicity while normal function type 1 dihedrals do. The function to write the atoms was further altered to be capable of setting the mass of both states of a bead to the highest mass of the two states if it is asked to do this, as shifting mass increases the risk of crashes during TI simulations especially in larger systems as mentioned earlier in the results. The function to write the dihedrals was further altered so that when the second state has a different multiplicity than the first state, the dihedral

will be split in two as GROMACS is not capable of altering the multiplicity of a dihedral for the Martini force field if the states shift during a TI simulation.
New functions(figure 7B) were added to read and write properties common to the Martini force field but for which functions were not yet present. The *ifdef FLEXIBLE* bonds, *ifndef FLEXIBLE* constraints and type(improper) dihedrals are added by their write functions to the bonds, contraints and dihedrals sections respectively. The exclusions and virtual sites n are given their own sections by their write functions. The functions to read the *ifdef FLEXIBLE* bonds and *ifndef FLEXIBLE* constraints require some additional explanation. The *define_flexible* function alters the *#ifdef FLEXIBLE* and *#ifndef FLEXIBLE* statements thereby preventing those bonds and constraints from being read, as they need to be handled separately because they need to be flanked by *#ifdef*/*#ifndef* and *#endif* statements[23]. Then the *read_flex* function reads both the *ifdef FLEXIBLE* bonds and *ifndef FLEXIBLE* constraints and uses independently defined function *equalize_flex_lists* to add any element present in those constraints but missing from the bonds to the *ifdef FLEXIBLE* bonds, it then stores all of those bonds.

The *Topology* class(figure 7B) shares its name with that of a class in *forcefield2.py* but has a different structure. The *Topology* class defined in *forcefield_martini.py* handles topology files and if it is a .top file will also contain all .itp files referenced in the .top which are not a standard part of the Martini3 force field. This makes this class capable of handling the hierarchical topologies of a .top files. The *self.main_topology* property is of the *TopolBase* class and contains the main .itp or .top, *self.main_has_atoms* indicates whether or not the main topology directly contains molecule definitions. The class had two functions *read_topologies* and *write_topologies*. The *read_topologies* function reads all .itp files referenced to in the main topology file and stores them in a list of TopolBase elements. The *write_topologies* function writes the main topology and all included .itp topologies under a consistent naming scheme. The *self.ffdir* refer to the name of the directory of the Martini3 force field. This property serfs to prevent standard components of the Martini3 force field reference in the main topology file from being unnecessarily read and stored.

martini_mutdb.py(figure 7B) has one class named *Mut_residue* to handle all atoms, bond, angles and dihedrals that need to have a second state added to them. The included function *read_mtp* reads all atoms, bond, angles and dihedrals for a hybrid residue from the file *mutres.mtp* in the force_field directory, but the function can be redirected to read another file. It is important to note that improper dihedrals need to be defined separately, this makes it easier to keep the oversight. The *update_idx_num* updates the IDs for the atoms and the residue to match those of the corresponding hybrid residue in the topology. The *update_BoAnDiIm* function uses the residue list from the topologies to add any atoms that lie outside the hybrid residue to the bonds, angles and dihedrals (both normal an improper), if the atom lies outside the scope of the molecule then the bond, angle or dihedral will be removed from the *Mut_residue* object as those do not exist in the topology. The independently defined function *add_second_states* uses a *mutres.mtp* file to add the second state for the atoms, bonds, angles and dihedrals for each hybrid residue. After all second states are added the update residues function is used to make the *self.residues* list anew with the second states present.

The *generate_hybrid_topology.py* script was altered to handle the new classes and functions for the martini force field. Any of the already existing flags aside from *-p*, *-ff* and *-o* will be ignored if the Martini force field is used. Two new flags were added for the Martini 3 force field. The *–mut* flag is a file options that if used will use the file under this flag instead of *mutres.mtp* in the force field directory. The -equalize-mass flag triggers the functionality in the write_atoms function that equalizes the masses of two states of the same atom.

shave_pdb.py(figure 7A) was made to remove the C and N from the names of the terminal residues and the D from the names of the dummy atoms in the pdb file. This needs to be done as otherwise the pdb file cannot be used by *martinize2*.

In order to use the pmx variant for the Martini 3.0.4 force field(figure 7A) first use *mutate.py* to generate a pdb with hybrid residues and then use the script *shave_pdb.py* to alter the pdb into something that can be used by martinize2. Afterwards martinize2 can be used to make Martini3 topology files out of the pdb. Then finally use the *generate_hybrid_topology.py* to add the second states to the topology files. Unless any beads unique to a specific all-atom force field are used the force field chosen doesn't really matter as any other details are not preserved by martinize2.

The Martini-pmx program made in this research from the standard pmx version can generate hybrid topologies for the Martini 3.0.4 force field. Currently this can only be done for mutation from serine to alanine and from serine to glutamate. In the future this will need to be expanded for all combination of canonical amino acids. To add a new hybrid residue to the force field it needs to be added at multiple places each in another way(figure S5). In addition in the future the code will need to be further streamlined to make it more efficient and compact. But if the repertoire of mutations is properly expanded and the code streamlined this would enable high throughput TI simulations as well as the generation of mutation libraries for the Martini 3.0.4 force field for a wide variety of simulated environmental conditions. It would also be wise to also make a version of pmx which can make GROMOS hybrid topologies in the future, so that the same can also be done for the GROMOS force field. This would allow high throughput TI simulations and mutation library generation for most of the commonly used force fields.

General discussion and conclusion

As mentioned in the introduction a recent article used MD simulations to show that SNARE mediated membrane fusion is an entropically driven process[14]. As mentioned in the results, mutations to alanine generally have a positive ΔΔG indicating that the mutations to alanine lower the free energy of folding. Thus this makes it more favorable for SNAREs to assemble. The reverse holds true for the mutations to glutamate and for phosphorylation as these cause a higher free energy of folding thus making SNARE assembly less favorable. This is a possible explanation for the observation by Malmersjö *et al*.[7] that mutations to alanine improve SNARE mediated membrane fusion while mutations to glutamate inhibit it.

The destabilizing glutamate mutations and phosphorylation have patterns of relative effects that mirrors that of the stabilizing alanine mutations. This means that when a residue has the most positive ΔΔG for a stabilizing mutation it also has a tendency to have the most negative ΔΔG for a destabilizing mutation. The implication of this is that certain residues have stronger effects when mutated than other residues. From the results this means that S54 has the strongest effect on the stability when mutated, followed by T47, although for the mutations to glutamate T47 can have a stronger effect for the AMBER force field and when shifting ions are used. T53 and S61 seem to have about equally strong effects although this seems to some degree dependent on the type of mutation. T47 is closer to S54 in value than it is to T53 for AMBER simulations of the mutations to glutamate, and is in fact with a few exception more negative than S54. However the reverse holds true for almost all other simulations of the mutations to glutamate. Overall the pattern of relative effects can be safely interpreted despite the sometimes large standard deviations, as with a few exceptions (mentioned in the results) the standard deviations almost never disrupted the pattern of relative effects. This pattern of relative effects is particularly interesting when compared to results from *Malmersjö et al.*[7](figure S6).There, just like in this research, mutating S54 to glutamate has a stronger effect on the relative secretion than T53 and T53 has

a weaker effect than T47. However unlike with *Malmersjö et al.*[7] T47 has stronger effect than S54 and S61 has the strongest effect in reducing the relative secretion while in this research it is generally the weakest. This is especially strange as T47E, T53E and S54E do not differ very strongly in relative secretion while S61E does. It has to be noted however that here the thermodynamics were calculated not the relative secretion like *Malmesjö et al.*[7] did. Also here only a piece of the SNARE complex was simulated instead of its entirety which means that in vivo S61 is not nearly as close the C-terminus as it is here. Regardless these differences will need to be further investigated in the future.

In case of the Martini force field using PME resulted into instabilities leading to core dumps, this means that under these conditions the martini simulations did not always make it to 6.2 ns but, with a few exception, always made to at least 4.2 ns. It has to be noted that for most simulations a few λ points made it to 6.2 ns while others did not. Most often the λ points 0 and 0.01 crashed but aside from that there were crashes for other λ points that happened in a seemingly random manner. Also the TE mutations with fc_1000000 did make it to 6.2ns for all λ points thanks to extra effort as the full length was required as the first 2 ns needed to be cut off, this was not done for the other simulations due to lack of time. Likely these instabilities are the result of the absence of a polarizable water model for the Martini 3 force field which is recommended when using PME. In future research making a polarizable water model for the Martini3 force field is thus highly recommended.

A combination of PME and shifting ions can largely but not completely reduce the difference between the GROMOS and AMBER force field for the GLU mutation. When combined with bigger box size it could reduce the difference between the GROMOS and Martini force fields for phosphorylation to its smallest point as well. PME also gave the smallest standard deviations for the Martini simulations of the mutations to alanine. Taken together this indicates that this is the best combination of settings that is used here. As mentioned in the results the use of a bigger box size and shifting ions make the differences between the split simulations and its non-split counterpart more or less disappear and is also a candidate for the smallest difference between GROMOS and AMBER for GLY-X-GLY mutations to glutamate. This indicates that a combination of a bigger box size, PME and shifting ions would give the best results but under those conditions the differences between the GROMOS and AMBER force fields are larger than when only PME and shifting ions are used both for ALA-X-ALA and GLY-X-GLY.

Thus as even at its lowest the differences between ΔΔGs of GROMOS and AMBER force fields is still significant for both the mutations to glutamate and to alanine(which always has the same but still significant difference). This can possibly be caused by the fact that AMBER uses an all-atom force field while GROMOS uses an united atom force field. This will need to be investigated into the future possibly by running the simulations performed here for another united atom and all-atom force field, possibly using CHARMM19[30,31] or OPLS-UA[32] for the united atom force field.

Considering there were significant difference between the ALA-X-ALA and GLY-X-GLY simulations, there is the question which one of the two gives the better results. In general the answer to this question it is unclear but there are several arguments in favor of both.
First the difference in relative effects patterns between Martini fc_100000 and fc_1000000 for phosphorylation is stronger with GLY-X-GLY than with ALA-X-ALA. The pattern of relative effects of fc_1000000 has with GLY-X-GLY phosphorylation is not consistent with the those of the GROMOS force field for mutations to glutamate and for phosphorylation (when the pattern is stable), while that of ALA-X-ALA is. Also ALA-X-ALA gives a better overlap between Martini fc_1000000 and GROMOS force fields for phosphorylation.

On the other hand the use of GLY-X-GLY tripeptides gives a decent match between GROMOS and AMBER force fields under both PME shifting ions and under shifting ions with bigger box size, while for ALA-X-ALA this is only the case with PME and shifting ions. Also the use of GLY-X-GLY tripeptides resulted in a more negative ΔΔG for phosphorylation in comparison to mutations to glutamate more often than the use of GLY-X-GLY tripeptides does. This taken together seems to indicate that the GLY-X-GLY give better results however this is not entirely clear and will need to investigated further in the future.

The fc_100000 simulations for Martini in general seem to give worse results than the fc_1000000 simulations. The fc_1000000 results in general seem to be much closer to those of either the GROMOS of AMBER force fields. This is not unsurprising as, using fc_1000000 for restricted bonds, was advised by the Martine force field itself. Thus the increase simulation speed is not worth the loss in accuracy. The Martini force field shows decent correlation with the GROMOS and AMBER force fields if fc_1000000 is used for restricted bonds. However even when fc_1000000 is used the ΔΔGs of the Martini force field are typically higher than those of GROMOS and AMBER. In addition the pattern of relative expression was different than those of the GROMOS and AMBER force fields for the mutations to glutamate. Also with the phosphorylation simulations the fc_1000000 variant was not much closer to the atomistic simulation than the fc_100000 variant except for GLY-X-GLY when shifting ions were used. It must be noted here however that the Martini3 force field is still being tested and optimized and is a coarse-grained force field meaning there are less beads and therefore less steric hindrance thus this might give higher ΔΔGs more easily.

So far the generated results are useful despite some outliers. As mentioned earlier in the discussion the current results provide a possible explanation for the observations made by Malmersjö *et al.*[7], thus the approach in itself seems to be useful. The methods performed in an attempt to fix the discrepancies (increasing the box size, using PME) between the GROMOS and AMBER force fields could partially but not fully reduce the difference between the GROMOS and AMBER force fields. Therefore attempts to fix the problems so far seems not be fully successful. Overall the research shows a possible explanation for the results of Malmersjö *et al.*[7], that Martini 3.0.4 produces results close to those of the atomistic simulations, and finally the fact that sometimes using somewhat different settings (lower force constant, using ALA-X-ALA instead of GLY-X-GLY) may significantly affect the results. A program called martini-pmx was made, which is capable of generating hybrid topologies for the Martini force field. It also has a force field which can do this. Also the Martini 3.0.4 force field was expanded to include phosphorylated threonine and serine.

References

1. Chen, Y. A. & Scheller, R. H. Snare-mediated membrane fusion. *Nature Reviews Molecular Cell Biology* **2**, 98–106 (2001).

2. Harbury, P. A. B. Springs and zippers: Coiled coils in SNARE-mediated membrane fusion. *Structure* **6**, 1487–1491 (1998).

3. Jahn, R., Lang, T. & Südhof, T. C. Membrane fusion. *Cell* **112**, 519–533 (2003).

4. Fasshauer, D., Sutton, R. B., Brunger, A. T. & Jahn, R. Conserved structural features of the synaptic fusion complex: SNARE proteins reclassified as Q- and R-SNAREs. *Proc. Natl. Acad. Sci. U. S. A.* **95**, 15781–15786 (1998).

5. Durrieu, M. P., Lavery, R. & Baaden, M. Interactions between neuronal fusion proteins explored by molecular dynamics. *Biophys. J.* **94**, 3436–3446 (2008).

6. Antonin, W., Fasshauer, D., Becker, S., Jahn, R. & Schneider, T. R. Crystal structure of the endosomal

snare complex reveals common structural principles of all snares. *Nat. Struct. Biol.* **9**, 107–111 (2002).

7. Malmersjö, S. *et al.* Phosphorylation of residues inside the SNARE complex suppresses secretory vesicle fusion . *EMBO J.* **35**, 1810–1821 (2016).

8. Shimazaki, Y. *et al.* Phosphorylation of 25-kDa synaptosome-associated protein: Possible involvement in protein kinase C-mediated regulation of neurotransmitter release. *J. Biol. Chem.* **271**, 14548–14553 (1996).

9. Polgár, J., Lane, W. S., Chung, S. H., Houng, A. K. & Reed, G. L. Phosphorylation of SNAP-23 in Activated Human Platelets. *J. Biol. Chem.* **278**, 44369–44376 (2003).

10. Shu, Y., Liu, X., Yang, Y., Takahashi, M. & Gillis, K. D. Phosphorylation of SNAP-25 at Ser187 mediates enhancement of exocytosis by a phorbol ester in INS-1 cells. *J. Neurosci.* **28**, 21–30 (2008).

11. Hirling, H. & Scheller, R. H. Phosphorylation of synaptic vesicle proteins: Modulation of the αSNAP interaction with the core complex. *Proc. Natl. Acad. Sci. U. S. A.* **93**, 11945–11949 (1996).

12. Mangan, S. & Alon, U. Structure and function of the feed-forward loop network motif. *Proc. Natl. Acad. Sci. U. S. A.* **100**, 11980–11985 (2003).

13. Atlashkin, V. *et al.* Deletion of the SNARE vti1b in Mice Results in the Loss of a Single SNARE Partner, Syntaxin 8. *Mol. Cell. Biol.* **23**, 5198–5207 (2003).

14. McDargh, Z. A., Polley, A. & O'Shaughnessy, B. SNARE-mediated membrane fusion is a two-stage process driven by entropic forces. *FEBS Lett.* **592**, 3504–3515 (2018).

15. Pronk, S. *et al.* GROMACS 4.5: a high-throughput and highly parallel open source molecular simulation toolkit. *Bioinformatics* **29**, 845–854 (2013).

16. Abraham, M. J. *et al.* Gromacs: High performance molecular simulations through multi-level parallelism from laptops to supercomputers. *SoftwareX* **1**–**2**, 19–25 (2015).

17. Leach, A. R. Ligand-based approaches: Core molecular modeling. in *Comprehensive Medicinal Chemistry II* **4**, 87–118 (Elsevier Ltd., 2006).

18. Pitman, M. R. & Menz, R. I. Methods for protein homology modelling. in *Applied Mycology and Biotechnology* **6**, 37–59 (Elsevier, 2006).

19. Gamini, R. & Chandler, D. *Residue-Based Coarse Graining using MARTINI Force Field in NAMD*.

20. Baron, R. *et al.* Comparison of thermodynamic properties of coarse-grained and atomic-level simulation models. *ChemPhysChem* **8**, 452–461 (2007).

21. Peregrine Documentation [HPC Documentation]. Available at: https://wiki.hpc.rug.nl/peregrine/start. (Accessed: 1st July 2020)

22. Seeliger, D. & de Groot, B. L. Protein thermostability calculations using alchemical free energy simulations. *Biophys. J.* **98**, 2309–2316 (2010).

23. Souza, P. C. T. *et al.* Martini 3.0: A General Purpose Force Field for Coarse-Grain Molecular Dynamics. (2020).

24. Schmid, N. *et al.* Definition and testing of the GROMOS force-field versions 54A7 and 54B7. *Eur. Biophys. J.* **40**, 843–856 (2011).

25. Lindorff-Larsen, K. *et al.* Improved side-chain torsion potentials for the Amber ff99SB protein force

field. *Proteins Struct. Funct. Bioinforma.* **78**, NA-NA (2010).

26. Marrink, S. J., Risselada, H. J., Yefimov, S., Tieleman, D. P. & De Vries, A. H. The MARTINI force field: Coarse grained model for biomolecular simulations. *J. Phys. Chem. B* **111**, 7812–7824 (2007).

27. Marrink, S. J. Parametrizing a new molecule. Available at: http://www.cgmartini.nl/index.php/tutorials-general-introduction-gmx5/parametrzining-new-molecule-gmx5. (Accessed: 26th March 2020)

28. Khoury, G. A., Thompson, J. P., Smadbeck, J., Kieslich, C. A. & Floudas, C. A. Forcefield_PTM: *Ab Initio* Charge and AMBER Forcefield Parameters for Frequently Occurring Post-Translational Modifications. *J. Chem. Theory Comput.* **9**, 5653–5674 (2013).

29. Khoury, G. A. *et al.* Forcefield_NCAA: *Ab Initio* Charge Parameters to Aid in the Discovery and Design of Therapeutic Proteins and Peptides with Unnatural Amino Acids and Their Application to Complement Inhibitors of the Compstatin Family. *ACS Synth. Biol.* **3**, 855–869 (2014).

30. Neria, E., Fischer, S. & Karplus, M. Simulation of activation free energies in molecular systems. *J. Chem. Phys.* **105**, 1902–1921 (1996).

31. III, W. E. R. *Theoretical studies of hydrogen bonding, Ph.D. Thesis, Harvard University*. (1985).

32. Sakae, Y. & Okamoto, Y. Optimisation of OPLS–UA force-field parameters for protein systems using protein data bank. *Mol. Simul.* **36**, 1148–1156 (2010).

33. Martin, M. G. Comparison of the AMBER, CHARMM, COMPASS, GROMOS, OPLS, TraPPE and UFF force fields for prediction of vapor-liquid coexistence curves and liquid densities. *Fluid Phase Equilib.* **248**, 50–55 (2006).

34. Hornak, V. *et al.* Comparison of multiple amber force fields and development of improved protein backbone parameters. *Proteins: Structure, Function and Genetics* **65**, 712–725 (2006).

35. Monticelli, L. *et al.* The MARTINI coarse-grained force field: Extension to proteins. *J. Chem. Theory Comput.* **4**, 819–834 (2008).

36. Gapsys, V., Michielssens, S., Seeliger, D. & de Groot, B. L. pmx: Automated protein structure and topology generation for alchemical perturbations. *J. Comput. Chem.* **36**, 348–354 (2015).

37. pmx. Available at: http://pmx.mpibpc.mpg.de/. (Accessed: 19th February 2020)

38. GitHub - deGrootLab/pmx: Toolkit for free-energy calculation setup/analysis and biomolecular structure handling. Available at: https://github.com/deGrootLab/pmx. (Accessed: 9th June 2020)

39. Home · dseeliger/pmx Wiki · GitHub. Available at: https://github.com/dseeliger/pmx/wiki. (Accessed: 9th June 2020)

40. GROMACS. Welcome to the GROMACS documentation! — GROMACS 2018.1 documentation. (2018). Available at: http://manual.gromacs.org/documentation/2018.1/index.html. (Accessed: 6th April 2020)

41. Van Gunsteren, W. F. & Berendsen, H. J. C. *The GROMOS Software for (Bio)Molecular Simulation GROMOS87 Groningen Molecular Simulation (GROMOS) Library Manual*.

42. Van Gunsteren, W. F., Berendsen, H. J. C. & Rullmann, J. A. C. Inclusion of reaction fields in molecular dynamics: Application to liquid water. *Faraday Discuss. Chem. Soc.* **66**, 58–70 (1978).

43. Darden, T., York, D. & Pedersen, L. Particle mesh Ewald: An N·log(N) method for Ewald sums in large systems. *J. Chem. Phys.* **98**, 10089–10092 (1993).

44. LLC, S. The PyMOL Molecular Graphics System, Version 1.8. (2015).

45. DeLano, W. L. Pymol: An open-source molecular graphics tool. *CCP4 Newsl. Protein Crystallogr.* **40**, 82–92 (2002).

46. GitHub - marrink-lab/vermouth-martinize: Describe and apply transformation on molecular structures and topologies. Available at: https://github.com/marrink-lab/vermouth-martinize. (Accessed: 9th June 2020)

47. Gapsys, V. & de Groot, B. L. pmx Webserver: A User Friendly Interface for Alchemistry. *J. Chem. Inf. Model.* **57**, 109–114 (2017).

48. Gapsys, V., Michielssens, S., Seeliger, D. & de Groot, B. L. Accurate and Rigorous Prediction of the Changes in Protein Free Energies in a Large-Scale Mutation Scan. *Angew. Chemie Int. Ed.* **55**, 7364–7368 (2016).

49. Vienna-PTM 2.0. Available at: http://vienna-ptm.univie.ac.at/. (Accessed: 19th February 2020)

50. Margreitter, C., Petrov, D. & Zagrovic, B. Vienna-PTM web server: a toolkit for MD simulations of protein post-translational modifications. *Nucleic Acids Res.* **41**, W422–W426 (2013).

51. Petrov, D., Margreitter, C., Grandits, M., Oostenbrink, C. & Zagrovic, B. A Systematic Framework for Molecular Dynamics Simulations of Protein Post-Translational Modifications. *PLoS Comput. Biol.* **9**, e1003154 (2013).

52. Margreitter, C., Reif, M. M. & Oostenbrink, C. Update on phosphate and charged post-translationally modified amino acid parameters in the GROMOS force field. *J. Comput. Chem.* **38**, 714–720 (2017).

53. Bussi, G., Donadio, D. & Parrinello, M. Canonical sampling through velocity rescaling. *J. Chem. Phys.* **126**, 014101 (2007).

54. Braun, E., Moosavi, S. M. & Smit, B. Anomalous Effects of Velocity Rescaling Algorithms: The Flying Ice Cube Effect Revisited. *J. Chem. Theory Comput.* **14**, 5262–5272 (2018).

55. Berendsen, H. J. C., Postma, J. P. M., Van Gunsteren, W. F., Dinola, A. & Haak, J. R. Molecular dynamics with coupling to an external bath. *J. Chem. Phys.* **81**, 3684–3690 (1984).

56. Verlet, L. Computer 'experiments' on classical fluids. I. Thermodynamical properties of Lennard-Jones molecules. *Phys. Rev.* **159**, 98–103 (1967).

57. Martini 2.2. Available at: http://cgmartini.nl/index.php/224-m22. (Accessed: 6th April 2020)

58. De Jong, D. H. *et al.* Improved parameters for the martini coarse-grained protein force field. *J. Chem. Theory Comput.* **9**, 687–697 (2013).

59. Yesylevskyy, S. O., Schäfer, L. V., Sengupta, D. & Marrink, S. J. Polarizable water model for the coarse-grained MARTINI force field. *PLoS Comput. Biol.* **6**, 1–17 (2010).

60. Mutation free energy calculations. Available at: http://pmx.mpibpc.mpg.de/lugano2019_tutorial1/index.html. (Accessed: 9th June 2020)